Applied Catalysis A: General 505 (2015) 52–61

Contents lists available at ScienceDirect

Applied Catalysis A: General

journal homepage: www.elsevier.com/locate/apcata

An environmentally benign and low-cost approach to synthesis of thermally stable industrial catalyst Cu/SiO_2 for the hydrogenation of dimethyl oxalate to ethylene glycol

Tiberiu Popa[a], Yulong Zhang[b], Erlei Jin[a], Maohong Fan[a,c,d,*]

[a] Department of Chemical and Petroleum Engineering, University of Wyoming, 1000 East University Avenue, Laramie 82071, WY, USA
[b] Western Research Institute, 3474 North 3rd Street, Laramie 82072, WY, USA
[c] School of Energy Resources, University of Wyoming, 1000 East University Avenue, Laramie 82071, WW, USA
[d] School of Civil and Environmental Engineering, Georgia Institute of Technology, Mason Building, 790 Atlantic Drive, Atlanta 30332, GA, USA

ARTICLE INFO

Article history:
Received 1 May 2015
Received in revised form 17 July 2015
Accepted 20 July 2015
Available online 26 July 2015

Keywords:
Dimethyl oxalate hydrogenation catalyst
Ethylene glycol
Cu/SiO_2
Ammonium carbonate

ABSTRACT

This investigation focused on developing an environmentally benign approach to synthesis of nanostructured Cu/SiO_2 catalysts for hydrogenation of dimethyl oxalate (DMO) to ethylene glycol (EG). It was accomplished by using $(NH_4)_2CO_3$, instead of the conventional ammonia evaporation method, for making nanostructured Cu/SiO_2 exhibiting good performance for DMO conversion and EG selectivity in the desired temperature range, with increased temperature stability. The resulting catalysts were characterized for catalytic activity, optimal reaction temperature, specific surface area, crystalline structure, surface composition and the influence of sodium in support raw material. The new method generated active catalysts with improved thermal stability linked to better dimension control and more Cu_2O content, together with improved morphology of the supported copper particles.

1. Introduction

Large variations in oil prices have recently led to many economic issues for petrochemical industries. Upcoming possible CO_2 emissions regulations [1–3] may aggravate these issues. Therefore, seeking alternative raw materials for production of chemicals has become imperative, among these being coal, natural gas and biomass [4]. Syngas produced from these resources can be used for producing ethylene glycol (EG) in two steps [5]: CO oxidative coupling to dimethyl oxalate (DMO) [4] and hydrogenation of DMO to EG.

The reaction generating ethylene glycol (EG) occurs in two major steps [6,7], having as an intermediary methyl glycolate (MG):

$$CH_3OOCCOOCH_3 + 2H_2 \rightarrow CH_3OOCCH_2OH + CH_3OH \quad \Delta H_0 = -30.03\,\text{kJ/mol} \tag{R1}$$

$$CH_3OOCCH_2OH + 2H_2 \rightarrow HOCH_2CH_2OH + CH3OH \quad \Delta H_0 = -28.70\,\text{kJ/mol} \tag{R2}$$

The resulting EG can be further hydrogenated/dehydrated to ethanol:

$$HO\text{-}CH_2\text{-}CH_2\text{-}OH + H_2 \rightarrow CH_3\text{-}CH_2\text{-}OH + H_2O \quad \Delta H_0 = -87.20\,\text{kJ/mol} \tag{R3}$$

In addition, other products might be generated, such as 1,2-butanediol, ethane [6,8], etc.

The key to the second step of EG production is to find a high-performance and environmentally friendly catalyst, and thus avoid the use of the established copper/chromia (Cu/Cr_2O_3) catalyst. Although there are Ru-ligands homogenous catalysts with good catalytic activity, the separation of the catalysts from the products of reaction can be difficult [8–11], thus heterogeneous catalysts are preferred.

As catalysts used for DMO hydrogenation to EG, supported Au, Ag and Au-Ag catalysts have been developed, also with remarkable activity. However, because they can have 10 wt.% Ag (Ag/MCM41 [12]) and for Au-Ag combination 8 wt.% Au and 4.5 wt.% Ag (Au-Ag/SBA15 [13]), these might not be the best choice as industrial catalysts, particularly if a less expensive option is present, such as Cu/SiO_2 catalysts.

As catalysts used for DMO hydrogenation directly to ethanol, successful were Cu/Al_2O_3 prepared using sol–gel methods [14], Cu phyllosilicates prepared by ammonia evaporation hydrothermal

---

* Corresponding author at: Department of Chemical and Petroleum Engineering, University of Wyoming, 1000 East University Avenue, Laramie, WY 82071, USA. Tel.: +1 307 766 5633/404 385 4577.
E-mail addresses: mfan@uwyo.edu, mfan3@mail.gatech.edu (M. Fan).

http://dx.doi.org/10.1016/j.apcata.2015.07.026

(AEH) method [15] and copper-phyllosilicate core-sheath nanoreactor using hydrothermal methods [16].

This research is aimed at designing a method that can be scaled up for synthesis of Cu/SiO_2 as an industrial catalyst for dimethyl oxalate (DMO) hydrogenation to ethylene glycol (EG). Numerous synthesis methods were examined to select the most suitable catalysts, using several selection criteria; among these criteria are current and announced environmental regulations, regulations governing the transport and storage of the raw materials (e.g. ammonia), the number and content effluents requiring treatment, the practicality of the method and ease of synthesis, the ability for automation, and the activity and selectivity of the catalyst samples.

The conventional Cu/SiO_2 synthesis procedure includes formation of tetraamino cupric complex by mixing copper nitrate with ammonia solutions to pH ~11, the addition of silica sol to the resulting solution, and ammonia evaporation (AE), achieved by boiling the suspension until the pH reaches 6–7 for the precipitation of copper compounds [9,10]. This method was developed in order to generate smaller crystalline structures and a wider coverage of Cu compounds on the support, compared with incipient wetness impregnation methods [7,17], and became the common method of Cu compounds deposition on support [7,10,11,18–21]. However, this hydrothermal method has a number of shortcomings:

- The whole conventional catalyst preparation process takes four hours of mixing before the ammonia evaporation step, and then, although evaporation in our lab conditions is faster due to the lower local atmospheric pressure caused by altitude (~780 mbar), another three hours at 90 °C was required, followed by a filtration and washing step, which required another hour.
- The quality of the catalyst is very sensitive to boiling temperature of the ammonia evaporation operation. For example, Chen et al. obtained three different catalyst morphologies in the 60–100 °C range [10] and Yin et al. described the influence of temperature on texture and Cu species distribution [18].
- The process requires constant supervision and cannot be accelerated because of the risk of hot spots associated with water evaporation and overflow of the viscous suspensions.
- The method generates fumes with high concentration of ammonia during the ammonia evaporation step [9,22], which definitely poses problems for large batches, and the waste gas stream needs to be treated in order to limit its ammonia concentrations below 25 or 50 ppm [23].
- The hydrogenation of DMO, pure Cu/SiO_2 (i.e., without stabilizer additives) prepared with ammonia evaporation methods, showed marked deactivation after ~16 h at 200 °C [7,9,11], thus a method producing more stable structures is desirable.

There are several possible alternatives to the ammonia evaporation method:

- Incipient wetness impregnation of silica, using various soluble copper compounds. However, this method generates less active catalysts, due to large distributions of the copper particles [17] and Cu particles agglomeration at higher loading [18].
- Sol–gel methods give active catalysts, but they tend to be slow, sensitive to other influences [24,25], and preparation methods are complex, reducing reproducibility [18].
- Cationic exchange methods [17] and chemisorption hydrolysis [26] leading to only 11–12 wt.% Cu loading.
- An environmentally friendly method appears to be precipitation using urea decomposition. This method employs two main techniques. The first one starts at low pH [27,28], using fine silica or silica sol as sources of SiO_2 and a solution of copper nitrate, where the starting pH can be adjusted with nitric acid [27] to 1–2. The precipitation pH 6–7 (6.8 [27]) is obtained via urea decomposition by heating at ~80–90 °C, followed by hot filtration, precipitate washing with large quantities of water [28], or re-slurrying of filter cake and re-filtration [27]. The second technique uses urea decomposition [29,30], starting from basic pH, of a solution of copper nitrate with added ammonia, together with silica sol and urea, heating at 80 °C for four hours until the formation of the precipitate, which is again followed by hot filtration. However, the details of the mechanism of the decomposition process are complex and not well understood [31,32]. Further, the urea decomposition reaction is relatively slow and continues as well as during the filtration step, thus the process requires immediate filtration while in the preferred end-pH range, followed by very good washing process to remove urea [27,28]. For larger sizes filter cakes, this can generate uneven copper concentrations, and the structures generated also demonstrate large deactivation (with DMO conversions as low as 60% [29]) after 90 h [19] to 100 h [29] of reactions at 190 °C.
- Other methods attempted for the synthesis of ester hydrogenation catalysts involved precipitation using Na_2CO_3, NaOH [33–35], $NaHCO_3$, and KOH [35];
- $(NH4)_2CO_3$ was tried as coprecipitation agent for Cu-Zn-Si oxides/hydroxides system at pH = 8, but the product had low Cu coverage due to the formation of copper complex ($Cu(NH_3)_4{}^{2+}$). In addition, it was stated that "$(NH_4)_2CO_3$ is not a suitable precipitant for copper ions and $Cu_2Zn_1Si_1$-$(NH_4)_2CO_3$ catalyst is not worth studying" [35], which is surprising because urea hydrolysis at the end of the complicated mechanism generates precisely NH_3 and CO_2 [27,29–32].

The methods in use tend to be fairly complicated and sensitive to various influences. Consequently, a less complicated approach to the synthesis of the Cu/SiO_2 catalyst is desirable for scale-up and industrial utilization. The catalyst synthesis process should:

(1) Have the ability for automation.
(2) Generate effluents needing treatment that are low in number and toxicity.
(3) Generate catalysts having good performance on DMO conversion, good EG, MG and ethanol selectivity over the desired temperature range, with increased temperature stability.

2. Experimental

2.1. Catalyst preparation

The catalysts were prepared following multiple routes. Their designation contains the percent of copper in the fresh (unreduced and unused) catalyst, the raw material used as source of silica and the process used for precipitation. For example, a catalyst containing 20 wt.% copper using ammonia stabilized silica sol AS30 and using ammonium carbonate as synthesis route was designated 20Cu-AS30-AC. The deposition precipitation using ammonium carbonate and ammonia evaporation are described below; the methods using tetraethoxysilane (TEOS) through sol–gel approach are placed in the electronic supplementary material section.

Deposition–precipitation was employed using $(NH_3)_2CO_3$ as precipitation agent (deposition using ammonium carbonate – AC): 7.6 g $Cu(NO_3)_2{\cdot}xH_2O$ (Puratronic®, 99.999% – metals basis, Alfa Aesar) were dissolved in 26.25 g water and the pH was corrected to pH = 1 using nitric acid 69.0–70.0% (J.T. Baker "Nitric Acid, 69.0–70.0%, BAKER INSTRA-ANALYZED® Reagent"). Next, the appropriate quantities of support generating substances: silica sol (24.90 g LUDOX® AS-30 colloidal silica 30% ammonia stabilized or 25.15 g LUDOX®AM-30 colloidal silica 30%, sodium stabilized, silica in water, Sigma-Aldrich) were added and stirred for 30 min. Then $(NH_3)_2CO_3$ (ammonium carbonate, ACS reagent, NH3>30.0+%, Sigma-Aldrich) saturated solution was added slowly to end-pH 6–7. The resulting suspension containing the precipitate continued to be stirred for 4 h for crystals maturation, then it was filtered, washed and dried at 89 °C for 10 h, and the resulting materials were calcined in air at 450 °C for four hours. Finally, after cooling in desiccator, the catalyst was crushed and sieved, and the fractions 125–250 μm were used for catalytic testing; the resulting catalysts were denominated 20Cu-AS30-AC and 20Cu-AM30-AC, respectively.

Deposition–precipitation using NH_3 (ammonia evaporation-AE): 7.6 g of $Cu(NO_3)_2 \cdot xH_2O$ (Puratronic®, 99.999% – metals basis, Alfa Aesar) were dissolved in 26.25 g water, followed by adding ammonia solution (Ammonia, 30%, Baker) to pH = 10–11 and stirring another 30 min resulting in a blue solution. Then 24.90 g silica sol (Silica sol LUDOX® AS-30 colloidal silica 30% silica in water, ammonia stabilized, Sigma-Aldrich) were added and stirred for four more hours. After this period the temperature was raised to 90 °C for the evaporation of ammonia until pH 6–7, when precipitation occurred. The precipitates were filtered, washed, dried at 89 °C for 10 h and the resulting materials were calcined in air at 450 °C for four hours. Finally, after cooling in a desiccator, they were crushed and sieved, and the fractions 125–250 μm were used for catalytic testing. The resulting catalyst was denominated 20Cu-AS30-AE.

2.2. Characterization of catalysts

The total metal loading of the catalysts was analyzed by inductively coupled plasma spectrometry (ICP) using PerkinElmer Optima 8300 ICP-OES Spectrometer.

To obtain specific surface area of the selected catalyst, N_2 adsorption isotherms were performed on a volumetric system AutosorbIQ ASIQC0100-4 Quantachrome Instruments, using N_2 (5.0 UHP, US Welding) and He (5.0 UHP, US Welding) after a degassing procedure at 150 °C for 4 h.

X-ray diffraction (XRD) tests were performed on a Rigaku Smartlab X-ray diffractometer system in thin layer powder configuration, 2Theta/Theta mode, 20–100° range, 0.02° step, 1°/min scanning speed. The software used for refinements was CrystalSleuth/American Mineralogist Crystal Structure Database [36].

X-ray Photoelectron Spectroscopy (XPS) and X-Ray-Excited Auger Electron Spectroscopy (XAES) data was collected using a Kratos Axis Ultra DLD X-ray Photoelectron Spectrometer. It employs a monochromated Al K-alpha source running at 150 W. Survey scans were acquired at 80 eV pass energy at 1 eV resolution. High resolution elemental scans were acquired at 40 eV pass energy at a resolution of 0.05 eV. The reduced and used samples were stored in vials under Ar.

Temperature programmed reduction tests were performed on a AutosorbIQ ASIQC0100-4, Quantachrome Instruments, equipped with thermal conductivity detector (TCD), using a mixture of 5 vol.% H_2 (5.0 UHP, US Welding)–95 vol.% N_2 (5.0 UHP, US Welding) and He (5.0 UHP, US Welding). After one hour at 110 °C in He, the sample was cooled to 50 °C, then the gas was changed to 5 vol.% H_2–95 vol.% N_2 and, after stabilization, the temperature was raised at 5 °C/min to above 900 °C (typically to 950 °C). The mass of the sample was calculated to contain ~10 mg Cu, thus the mass of 20Cu-AS30-AC, 20Cu-AM30-AC and 20Cu-AS30-AE was ~0.05 g, equivalent samples containing 10 wt.%Cu/SiO_2 introduced had a mass of ~0.1 g.

The morphology and the particle size as well as the dispersion of the catalysts were studied by transmission electron microscopy (TEM) using FEI- Tecnai G2 F20 S-Twin 200 kV equipment. Samples for TEM observations were prepared by dispersing the catalysts in ethanol and drying one drop of the solution on copper grids. The particle size distribution was calculated on monolayer particles by using ImageJ 1.48v [37] and Icy 1.5.3.0 [38] software. The image analysis for particles in one layer in samples led to the dimensions of the particles; the shape factor used was circularity $f_{circ} = 4\pi A/P^2$ where A is the area of the shape and P is the perimeter of the shape (for a perfect circle this has value 1); the equivalent diameter d_e is Feret's diameter $d_e = \sqrt{P/\pi}$ where P is the perimeter of the shape.

2.3. Catalytic activity tests

The hydrogenation of dimethyl oxalate was performed on the experimental set-up shown in the schematic drawing Fig. S1. The system has four main gas lines (H_2, N_2, Ar and optional gas, shown at the top left corner of the drawing) with flow rates controlled by corresponding mass flow controllers, and a liquid injection line for DMO 10 wt.% in methanol (Dimethyl oxalate, 99%, VWR and Methanol, Certified ACS >99.8%, Fisher Chemical) with flow rate regulated by a high pressure pump (LabAlliance Series 1). H_2 (5.0 UHP, US Welding) was the reaction gas, N_2 (5.0 UHP, US Welding) was the carrier gas, while He (5.0 UHP, US Welding) or Ar (5.0 UHP, US Welding) served as internal gas standard. The reaction gases were supplied from pressurized gas cylinders by high pressure reducers, regulated by high pressure mass flow controllers (Parker-Porter), and then mixed with the vaporized liquid. The catalyst was synthesized in oxide form and required reduction four hours at 350 °C in H_2 before being used as catalyst for DMO hydrogenation. The DMO hydrogenation reaction occurred in a ½ inch fixed bed reactor with 11 mm inner diameter, and its temperature was set by a controller regulated furnace. The catalyst was introduced into the reactor without dilution with quartz sand and it was supported by inert material (ceramic wool). Gaseous products were analyzed by online gas chromatograph SRI 8610C, SRI Instruments, equipped with two Restek packed columns 1/8 in. × 6 in. (3.175 mm × 182.88 cm) Hayesep D and 1/8 in. × 6 in. (3.175 mm × 182.88 cm) MolSieve 13× and a capillary column 0.53 mm ID × 60 m × 5 μ Restek MXT-1, with a standard error ~5%, while liquid products were collected and analyzed by offline GC–MS Agilent 7890A-5975C VL MSD (mass spectrometer) using an Agilent HP-5MS (30 m × 0.250 mm) capillary column, equipped with Automatic Liquid Sampler (ALS) and standard error ~2%. The reaction system was controlled by a computer through a National Instruments DAQ system.

Test procedure: 1.51 g catalyst corresponding to 0.3 g Cu was loaded into the reactor with the thermocouple in the middle of the catalyst bed. The top and bottom of the catalyst bed was packed with inert material (ceramic wool). After leak check the system was pressurized with N_2 to the reaction pressure for additional leak check and the catalyst reduced in 92.6 vol.% H_2 and 7.4 vol.% N_2 at 350 °C for 4 h. After reduction step, the pressure and temperature were set to test parameters and 10 wt.% DMO/methanol was introduced. During testing, the pressure was maintained at specified pressure and the lowest test temperature of 170 °C (above the vaporization temperature of DMO), and the maximum temperature was established as selectivity to EG and MG decreased to less than ~30%, typically 240 °C, while 20Cu-AM30-AC was tested up to 260 °C. The test conditions were: catalyst mass corresponding to 0.3 g Cu, pressure 2 or 3 MPa, temperature at least 170 °C, weight hourly space velocity (WHSV) 0.8 (g DMO/(h*g cat.)), 92.6 vol.% H_2, 7.4 vol.% N_2, H_2/DMO mol ratio 80/1, 10 wt.% DMO/methanol. Gas products were analyzed by inline GC and liquid products were collected from sample cylinder at specified intervals (typically every hour) and analyzed by offline GC–MS.

After analysis of the liquid fraction using GC–MS, data was used to generate values for DMO conversion, selectivity and yield values to EG, MG, ethanol, and also molar flow rates of the analyzed products. From reactions (R1) to (R3) it can be observed that 2 mol H_2 are consumed to hydrogenate 1 mol DMO to produce 1 mol MG, 4 mol

H_2 are consumed for 1 mol DMO generating 1 mol EG and 5 mol H_2 for 1 mol DMO is required to generate 1 mol ethanol. Knowing the flow rate of DMO it means catalytic activity of the hydrogenation catalyst can be expressed in terms of (mol H_2/(h*g cat)) used to generate EG, MG and ethanol thus eliminating the influence of other side-reactions (thermal decompositions, intra and inter-molecular dehydrations, etc.) in the analysis of the hydrogenation catalysts.

3. Results and discussion

3.1. Characteristics of the catalysts

One important issue of earlier attempts to use ammonium carbonate was the large loss in copper during precipitation step, making the concentration of copper compounds very low in comparison with the other methods [35]. Table 1 shows the results of ICP-OES for metals loading and it demonstrates that, when using ammonium carbonate, the precipitate copper content is similar to the sample prepared by the ammonia evaporation method. The concentrations of Cu in prepared catalysts are similar with those reported in literature for other methods [10,18,28].

BET analyses (Table 2) show that the catalyst obtained using ammonia evaporation has the highest surface area for the fresh catalyst (334.817 m^2/g), but after ~16 h at high temperature (4 h, 350 °C reduction in H_2 then above 170 °C in DMO-H_2 stream) the catalyst loses 35.45% from the initial specific surface area, while in the case of the AC precipitation the catalyst 20Cu-AS30-AC loses 28.01% under the same conditions, while 20Cu-AM30-AC starts with the lowest specific surface area (150.0 m^2/g) and also loses 22.4% of the initial specific surface area.

XRD patterns obtained for the unreduced (fresh), reduced and used catalyst show the growth of metal crystalline phase for the used catalysts, and confirms sintering as one of the deactivation mechanisms. Fig. 1 shows the XRD patterns obtained for the unreduced (fresh) samples as they resulted after calcination in air for 4 h at 450 °C in the form intensity vs. 2θ. The sample obtained by ammonia evaporation technique using the ammonia stabilized silica sol (20Cu-AS30-AE-fresh) displays less evident peaks, signifying less crystallinity compared with the other two samples. The large peak centered near 23° can be assigned to poorly crystalized SiO_2 structures [21,24,39]. All three samples display this peak, while the rest of the larger peaks displayed by the samples can be assigned to CuO (tenorite) [21,24,39] and some small peaks can be assigned to copper silicates [10]. As can be seen in Fig. 1, the crystallinity of the samples is in order from more crystalline to less crystalline: 20Cu-AS30-AC-fresh > 20Cu-AM30-AC-fresh > 20Cu-AS30-AE-fresh. In the case of the catalyst prepared using the Na^+ stabilized silica sol, the XRD spectra suggests it depressed the proper crystallization of tenorite (CuO) during precipitation.

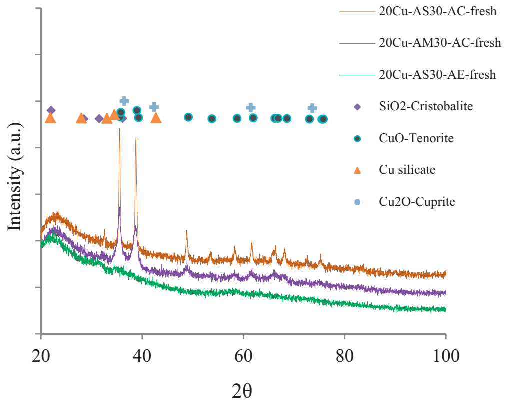

Fig. 1. XRD spectra for fresh 20Cu-AS30-AC, 20Cu-AM30-AC and 20Cu-AS30-AE.

Table 1
Total loading as determined by ICP-OES.

Sample	Cu (wt.%)	Na (wt.%)	Si (wt.%)	Cu/Si (wt/wt)
20Cu-AS30-AC fresh	18.37	0.03	35.97	0.5
20Cu-AS30-AC used 200 h	18.16	0.05	36.08	0.5
20Cu-AM30-AC fresh	18.67	0.14	35.73	0.5
20Cu-AM30-AC used 200 h	19.08	0.14	35.55	0.5
20Cu-AS30-AE fresh	18.14	0.02	36.12	0.5
20Cu-AS30-AE used 16 h	18.38	0.02	35.98	0.5

Table 2
Specific surface areas for the fresh and used catalysts.

Sample	BET surface area (m^2/g)	BJH total pore volume (cm^3/g)	BJH average pore diameter (nm)
20Cu-AS30-AC fresh	215.6	0.509	9.52
20Cu-AM30-AC fresh	150.0	0.873	12.25
20Cu-AS30-AE fresh	334.8	1.187	3.04
20Cu-AS30-AC used	155.2	0.420	12.17
20Cu-AM30-AC used	116.4	0.720	12.25
20Cu-AS30-AE used	216.1	0.902	3.40

Fig. S4 and S5 illustrate the spectra of the XRD test for reduced and for used catalysts. The large peaks at ~43.4°, 50.6° and 74° can be assigned to metallic Cu (Cu^0), while the peak at 36.5° and the wide peak centered around 61.5° can be assigned to cuprite (Cu_2O as mineral-cuprite has largest peak at 36.46° and other large peaks at 42.35°, 61.44° and 73.6°). Compared to the peaks generated by metallic Cu, the cuprite peaks are much wider, signifying a poorly crystalline and small crystal domains phase. Comparing spectra of the catalysts, it can be seen that in the case of the catalyst prepared using ammonia evaporation, the peaks for Cu^0 are much smaller, compared with the catalyst prepared using ammonium carbonate precipitations, signifying smaller crystalline size, while the peaks assigned to cuprite tend to be much larger. The catalyst prepared using Na^+ stabilized silica sol (AM30) displays initially a larger cuprite wide peak at ~36.5° after reduction, but after use it shows peaks similar to the peaks generated by the other catalyst prepared using ammonium carbonate precipitation.

The values generated using Scherrer's equation (Table 3) for all catalysts tested illustrate larger Cu^0 particles for the reduced and used catalyst compared with the CuO particles of the fresh catalyst suggesting a sintering process. Cu_2O peaks were very broad and could not be analyzed, which underlines the difficulty of XRD analysis for systems having mixed crystalline with almost amorphous/vitreous structures, where the amorphous fraction does not have enough regularly repeated atomic layers to generate by interference significant XRD signal, and reveals that for Cu_2O component XRD might not be the most suitable technique.

Temperature programmed reduction (TPR-H_2) test results for the fresh (unreduced and unused) samples are shown in Fig. 2. For the sample 20Cu-AS30-AE it shows only one peak at 240 °C, corresponding to reduction of the finely disseminated CuO [10,26], while the sample containing half the metal coverage, but having the same quantity of metal (~10 mg Cu) in the sample introduced in the test equipment, shows also one relatively sharp peak but at lower temperature (226 °C) In the case of 20Cu-AS30-AC there are two features, one peak representing a maximum of H_2 consumption at

Table 3
Crystal dimensions determined using Scherrer equation.

Catalyst	20Cu-AS30-AC			20Cu-AM30-AC			20Cu-AS30-AE		
	Fresh	Reduced	Used	Fresh	Reduced	Used	Fresh	Reduced	Used
Particle	CuO	Cu^0	Cu^0	CuO	Cu^0	Cu^0	CuO	Cu^0	Cu^0
Size (nm)	13.98	31.90	31.92	8.80	23.52	24.82	4.71	3.45	3.52

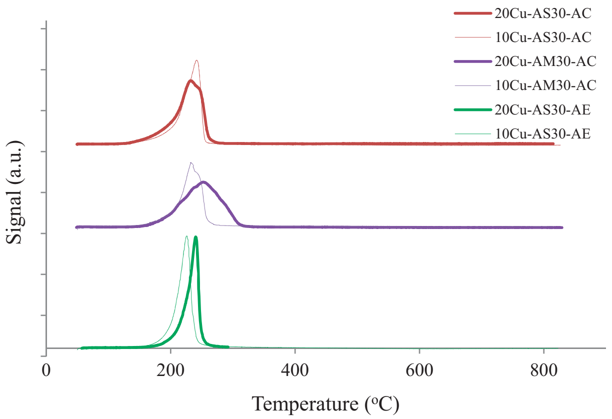

Fig. 2. TPR of the 20Cu-AS30-AC, 10Cu-AS30-AC, 20Cu-AM30-AC, 10Cu-AM30-AC, 20Cu-AS30-AE and 10Cu-AS30-AE (~10 mg Cu, 5 vol.% H_2 balance N_2, 5 °C/min).

232 °C, corresponding to the reduction of finely disseminated CuO on support [10,26], and a shoulder at 248 °C, corresponding to the reduction of bulk CuO in the structure [10,26] while 10Cu-AS30-AC has one peak at 242 °C. The sample 20Cu-AM30-AC shows one peak centered at 249 °C with a possible small shoulder at 236 °C while 10Cu-AM30-AC has the main peak at 226 °C and a shoulder at 244 °C.

XPS/XAES tests results illustrated in Fig. 3 give more information about the composition to an analysis depth of a maximum 20 nm [40]. The peaks centered at 933 eV binding energy (Cu2p), representing Cu in terms of Cu wt.% on the surface (Fig. 3a), can be deconvoluted into peaks representing Cu^{2+}, but the peaks position (binding energy) for the Cu^0 and Cu^{1+} are almost identical [30]. To obtain the concentration values for Cu^0 and Cu^{1+}, the XAES Cu LMN spectra were used (Fig. 3b), and the results of the combined XPS/XAES tests are shown in Table 4. The surface of calcined 20Cu-AS30-AE has 27.76 Cu wt.% as 23.76 wt.% Cu^{2+}, but also 4 wt.% Cu^+, suggesting that some tetraamino cupric material was encapsulated in silica gel [24] and during calcination its decomposition generated a reductive environment, but the value obtained by XPS is larger than the value obtained from ICP suggesting that most of copper compounds are on the surface of the support. Secondly, the dispersion of the total copper on the silica support drops by almost 50% from initial value (13.89 wt.%) after the reduction step at 350 °C in hydrogen, although the decomposition of copper silicate and copper migration during reduction should make available more copper materials [10]. Thirdly, after an additional ~8 h in-stream the coverage becomes only 46.1% of the original coverage (12.79 wt.%) because of sintering. In contrast, for the AC prepared catalysts, in the case of fresh 20Cu-AS30-AC, Cu coverage (11.51 wt.%) is lower than the value obtained using ICP suggesting that a large fraction is below the surface, also copper is more reduced after calcination step suggesting encapsulation, a similar case being observed for 20Cu-AM30-AC-fresh where part of total Cu (10.77 wt.%) could be attributed also to more reduced copper. Copper coverage for 20Cu-AS30-AC catalyst can be estimated at only 41.5% of the Cu wt.% coverage of the AE prepared catalyst, meaning that Cu concentrates in three-dimensional structures instead of layers, which is in agreement with TEM. Further, XRD shows that compared to 20Cu-AS30-AE, AC based catalysts have sharper peaks, meaning more compact and better crystallized CuO in the case of fresh catalysts.

This translates into better crystallized Cu^0 phases after reduction, a process that is slightly depressed by Na^+ in 20Cu-AM30-AC. However, XPS results show that in reduced and used catalysts the majority of copper is Cu^+, with Cu^{2+} also having a significant fraction, likely as copper silicates. Additionally, XPS data show that, for AC prepared catalysts, the effect of the partial decomposition of copper silicate and the following copper migration during reduction offsets sintering. However, after being used, the copper coverage decreases again, but only at about 72.9% of the original coverage for 20Cu-AS30-AC and just at 96.5% of the original coverage for 20Cu-AM30-AC.

As can be seen from TEM images (Fig. 4), the catalysts obtained using ammonia evaporation (AE) differ in morphology from both silica support particles (light gray) and also in the deposited copper containing material (dark gray), from the catalysts generated using ammonium carbonate precipitation. The supported material morphology in 20Cu-AS30-AE fresh sample is widely distributed on support at nanometer size and largely featureless, which prevented obtaining proper images required for the particle identification. Although XRD is unreliable for poorly crystalized materials as is 20Cu-AS30-AE fresh sample, a value of 4.71 nm diameter was obtained for CuO using the peak at $2\theta = 58.7°$. The material covering the silica starts aggregating during reduction after four hours at 350 °C in ~3.3 nm structures, and it will accumulate in masses of uneven size and an equivalent mean value diameter d_e of 3.0 nm for the used catalysts. In the case of the AC samples, the supported material is concentrated in smaller regions of almost round shape with $d_e = 2.8$ nm, and the structures become 2.9 nm after reduction, as sintering occurs. The catalyst used in-stream shows aggregates of around 3.9 nm. The morphology of the support differs; while AC samples have rounded supporting silica structures, the AE samples were elongated, some slab-like, but, after use, the morphology changes into more round structures. It is possible that this behavior is due to the partial decomposition of phyllosilicate during reduction and reconstruction of the structures of copper oxides, silica and again phyllosilicate during use or because of the substance loss due to the reaction with methanol generating the observed tetramethoxysilane [10].

3.2. Effect of different factors on dimethyl oxalate hydrogenation

3.2.1. Pressure and temperature

For this research, published and new methods were used to generate 20 wt.% Cu/SiO_2 catalysts, which were tested using the same method using catalyst mass corresponding to 0.3 g Cu and reactor pressure: 2 MPa (Fig. S2 and S3). The activity of the catalysts was analyzed as function of the DMO conversion and catalytic activity toward the economically desirable EG, MG and ethanol.

In terms of DMO conversion as a function of temperature, the catalyst prepared using AS-30 silica sol (ammonia stabilized) as support and precipitation using ammonium carbonate at end-pH 6–7 was very active, and maintained good activity after 14–16 h on-stream, while most of the unstabilized AE prepared Cu/SiO_2 catalysts in the literature reported loss of activity after 10–16 h on-stream [7,9,11]. A catalyst with the same raw material as

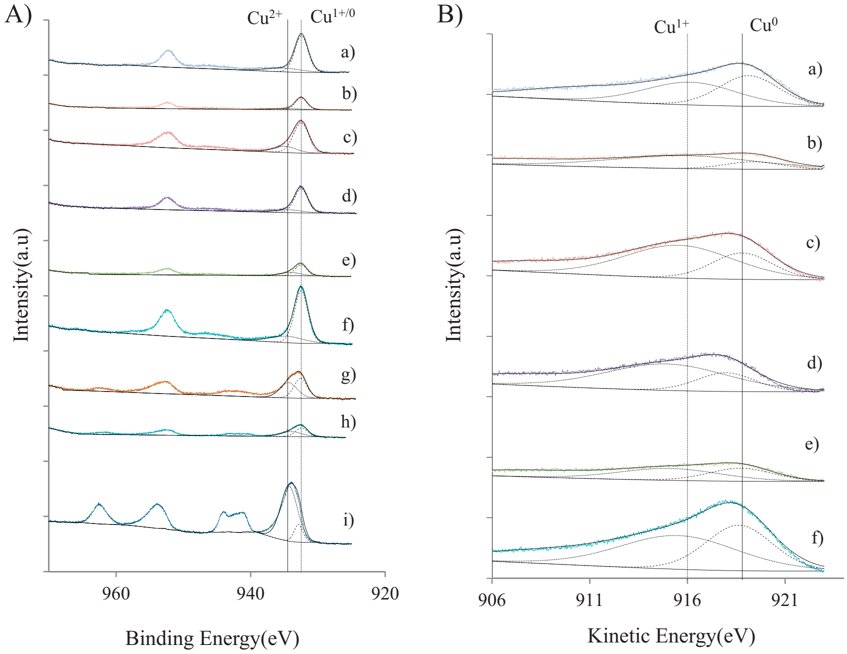

Fig. 3. (A) XPS Cu 2p spectra of the catalysts; (B) XAES Cu LMN spectra of the reduced and used catalysts; (a) 20Cu-AS30-AC used, (b) 20Cu-AM30-AC used, (c) 20Cu-AS30-AE used, (d) 20Cu-AS30-AC reduced, (e) 20Cu-AM30-AC reduced, (f) 20Cu-AS30-AE reduced, (g) 20Cu-AS30-AC fresh, (h) 20Cu-AM30-AC fresh, (i) 20Cu-AS30-AE fresh.

Table 4
Atom coverage (wt.%) on the catalyst surfaces resulting from XPS (Cu 2p peak) deconvolution.

wt.%	Catalyst								
	20Cu-AS30-AC			20Cu-AM30-AC			20Cu-AS30-AE		
	Fresh	Reduced	Used	Fresh	Reduced	Used	Fresh	Reduced	Used
Cu^{2+}	5.79	2.56	1.80	5.46	4.26	2.37	23.76	3.21	3.03
Cu^{1+}	4.97	7.87	3.55	4.43	4.95	6.58	4.00	6.09	6.78
Cu^{0}	0.63	2.62	3.07	0.88	3.74	1.45	0.00	4.59	2.98
Total Cu(2p)	11.51	13.05	8.39	10.77	12.95	10.40	27.76	13.89	12.79

20Cu-AS30-AC, but having end-pH 5.5 showed lower conversion, signifying the optimal end-pH is 6–7; above pH = 7 there were Cu loses in filtrate.

Plotting the result in terms of catalytic activity to desirable products (mol H_2/(h*g cat.)), the tests at 2 MPa shows that 20Cu-AS30-AC at 210 °C is 9.56% more active than 20Cu-AS30-AE at its highest activity (200 °C) while 20Cu-AM30-AC at 210 °C is 5.18% less active than the AE prepared catalyst at 200 °C.

Above 220 °C byproducts were identified as traces of methyl acetate, methylal, 1-propanol, 2-butanol, 2-methyl-1-butanol, acetic acid, methoxy-methyl ester, 1,2-butanediol etc. As temperature increased above 200 °C, tetramethoxysilane (TMOS) was also detected in liquid phase, but as the test advanced, TMOS quantity decreased, although still within the detection limit of the GC–MS. As the temperature increased above 200 °C, the gaseous products increasingly showed CO and CO_2 from 210 °C, a sign of the onset of decomposition, excessive hydrogenation/dehydration (ethane, methane), molecular and/or intermolecular dehydration (ethylene, dimethyl ether).

The results of these preliminary tests showed that catalysts prepared using ammonia carbonate precipitation and silica sol AS-30 performed very well, both in terms of EG and MG selectivity and DMO conversion. The catalysts precipitated using ammonium carbonate at end-pH 6–7 using ammonia stabilized silica sol (20Cu-AS30-AC) was selected, to test the effect of increased quantities of sodium in the structure the catalyst prepared using sodium stabilized AM-30 colloidal silica (20Cu-AM-AC) and for comparison purposes the catalyst prepared using ammonia evaporation (20CuAS30-AE), were the object of further investigations.

The evaluation tests of the catalysts prepared with both AC and AE methods were performed with a set-up similar with the installation shown in Fig. S1, but equipped for 3 MPa. The conditions were the same as used previously, but a pressure of 3 MPa was employed.

Fig. 5 shows that the performance of the catalysts prepared with conventional AE method and the new AC method are significantly different. The DMO conversions achieved with 20Cu-AS30-AE catalyst reached 90% or higher percentages when reaction temperatures were above 200 °C, Further, at 190 °C, the DMO conversion of 20Cu-AS30-AC is already as high as 96.4%, higher than that of 20Cu-AS30-AE, and with a yield of EG of 76.36%, compared with the value of 28.86% in the case of 20Cu-AS30-AE. 20Cu-AS30-AC is substantially improved over that prepared using AE, both in terms of DMO conversion and EG and MG selectivity. Furthermore, 20Cu-AS30-AC also exhibits an increase in selectivity to EG over a wider temperature range. The catalyst 20Cu-AM30-AC has lower conversion at the same temperature, but it also shows reduced ethanol production. It reaches a maximum yield of EG at 230 °C which may be attributed to the 0.1% sodium content in the silica sol used to generate the support, pointing to the role of the support in modulating the catalytic reaction [19].

3.2.2. Thermal stability

According to literature [11,19,29], pure Cu/SiO_2 (i.e., without stabilizer additives) for the hydrogenation of DMO, prepared with

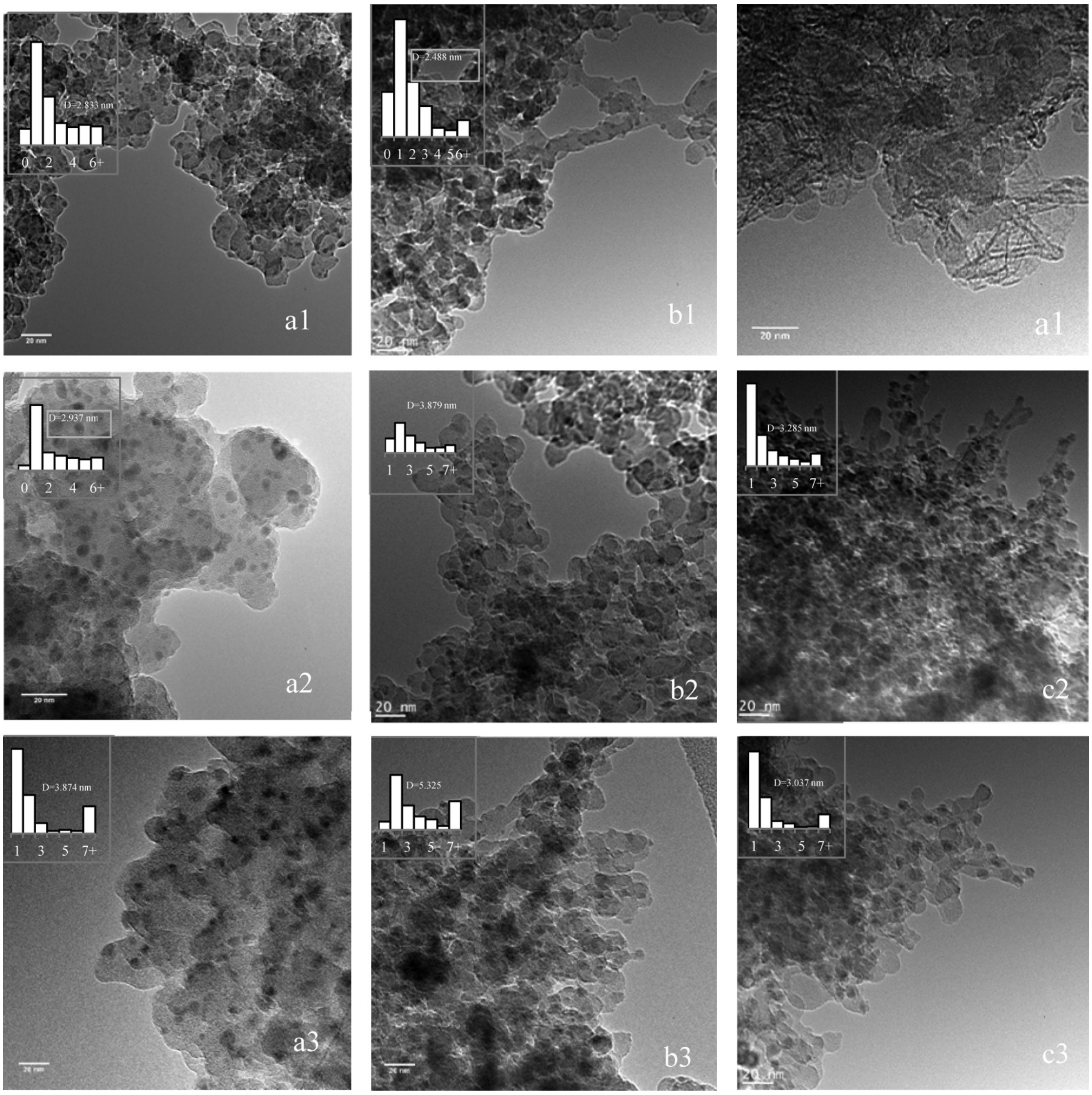

Fig. 4. TEM images of Cu/SiO_2 catalysts (a) 20Cu-AS30-AC; (b) 20Cu-AM30-AC; (c) 20Cu-AS30-AE: (1) fresh, (2) reduced, (3) used.

ammonia evaporation methods, showed markedly deactivation after ~16 h at 200 °C [7,9,11]. In addition, Cu/SiO_2 prepared though urea decomposition had considerable deactivation (with DMO conversions as low as 60% [29]) after 90 [19] to 100 [29] hours of reaction at 190 °C. A thermal stability test for 20Cu-AS30-AC was performed at 2 MPa and 210 °C for 200 h, and is illustrated in Figs. 6 and 7. Scattering of the results is attributed to the pressure variation associated with collecting samples, but the behavior of the catalyst remained stable. The result of the test (Fig. 6) indicates that the conversions of DMO with the catalyst 20Cu-AS30-AC prepared in this research only decrease from 99.5% to 97.5%, even after 200 h, and the selectivity to EG decreases from 85.5% only to 79%. The better performance of 20Cu-AS30-AC is attributed to the compact nanosized crystalline copper structures containing a large fraction of Cu^+ and low Cu coverage between Cu regions, which can reduce Cu migration and thus the deactivation of the catalyst due to sintering [33]. As can be observed, the catalytic activity, expressed as mol H_2/(h*g cat.) for the production of EG, MG and EtOH (Fig. 7), remains almost constant, mainly because as the test advanced the quantity of ethanol decreased in favor of the production of MG, while EG selectivity remained almost constant.

In the case of the 20Cu-AM30-AC, the test for thermal deactivation was also performed, at the temperature of maximum activity 230 °C and 2 MPa and is illustrated in Figs. 8 and 9. Although the catalyst had very good DMO conversion during the entire test, as presented in Fig. 8, the catalyst started showing signs of deactivation after only ~85 h in-stream, when it also showed increased sensitivity to the pressure variation in the test installation associated with collecting samples, resulting in an increased scattering of the results.

The deactivation is more pronounced as it is analyzed in terms of catalytic activity toward EG, MG and ethanol expressed as mol H_2/(h*g cat) and illustrated in Fig. 9, which shows not only a delay in reaching maximum activity, but also a pronounced loss of more than 17% from the maximum activity after 200 h.

Both catalysts produced using AC method performed better than the catalyst produced using AE method, which was also tested at 210 °C and 2 MPa (Figs. 10 and 11), which, as expected [7,9,11], displays the onset of deactivation marked by the decrease in DMO conversion after 15 h at 210 °C.

Weight liquid hourly space velocity (*WLHSV*) tests in the range 0.2–4.2 h^{-1} were performed at 3 MPa and 210 °C for 20Cu-AS30-AC (Figs. 12 and 13), and 3 MPa and 230 °C in the case of

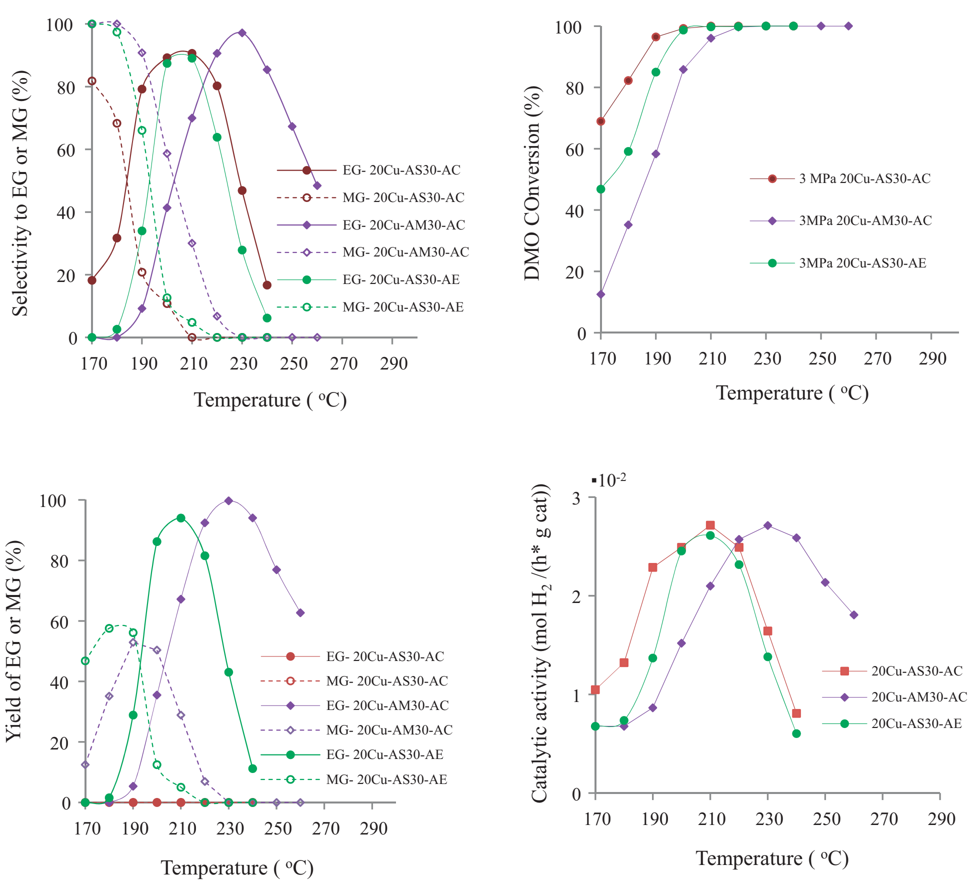

Fig. 5. The performances of the 20 wt.% Cu/SiO$_2$ catalysts prepared with conventional and new methods (a) selectivity to EG and MG; (b) DMO conversion; (c) yield of EG and MG; (d) catalytic activity to EG + MG + Ethanol [catalyst mass: 0.3 g Cu, gas condition (pressure: 3 MPa; WHSV: 0.8 g DMO/(h*g cat.); H$_2$: 92.6 vol.%; N2: 7.4 vol.%); H$_2$/DMO mol ratio: 80/1].

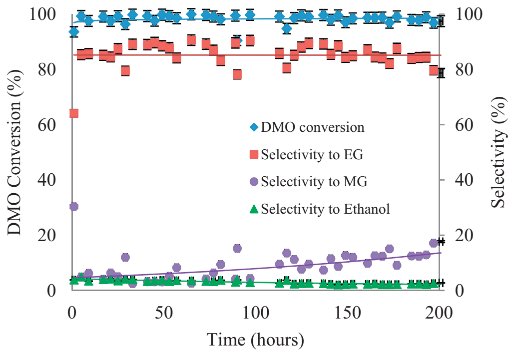

Fig. 6. Stability test of 20Cu-AS30-AC [catalyst mass: 0.3 g Cu, gas condition (pressure: 2 MPa; WHSV: 0.8 g DMO/(h*g cat.); H$_2$: 92.6 vol.%; N$_2$: 7.4 vol.%); H$_2$/DMO mol ratio: 80/1, 210 °C].

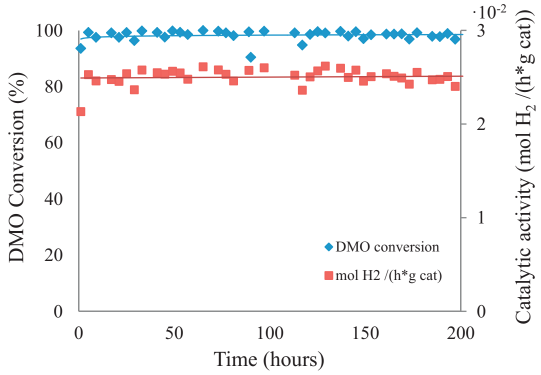

Fig. 7. Stability test of 20Cu-AS30-AC as DMO conversion and catalytic activity to EG + MG + ethanol [catalyst mass: 0.3 g Cu, gas condition (pressure: 2 MPa; WHSV: 0.8 g DMO/(h*g cat.); H$_2$: 92.6 vol.%; N$_2$: 7.4 vol.%); H$_2$/DMO mol ratio: 80/1, 210 °C].

20Cu-AM30-AC (Figs. 14 and 15). As can be seen from figures, the catalysts performed better at higher values of WLHSV due to the reduction in over-hydrogenation of the EG produced connected to the production of ethanol. At WLHSV 4.2 h^{-1} the DMO conversion was still 100% in the case of both catalysts prepared using ammonium carbonate methods and selectivity to EG reached 94.22% at 3.9 h^{-1} in the case of 20Cu-AS30-AC and 97.2% at 4.2 h^{-1} using 20Cu-AM30-AC. Analysing the hydrogenation catalysts in term of catalytic activity toward EG, MG and ethanol (mol H$_2$/(h*g cat)) both 20Cu-AS30-AC (Fig. 13) and 20Cu-AM30-AC (Fig. 15) show a surprisingly straight line, signifying additional unused catalytic capabilities, but possibly at lower EG selectivity.

The method using ammonium carbonate, besides being much faster and with results only tied to end-pH, gives characteristics more desirable for industrial use, for which this class of catalysts is aimed. The method also produced comparably more active catalysts. The analysis of the material is somewhat surprising. TPR suggests the presence of a CuO bulk phase for the more active 20Cu-AS30-AC, while only one peak for the similar catalyst prepared using AE. The XRD also shows the presence of well crystalized CuO in the case of fresh (unused and unreduced) 20Cu-AS30-AC, with tall and narrow Cu peaks for both the reduced and used catalyst. Different morphology, compared with the catalyst prepared using ammonia evaporation, is exposed by TEM. There is more free

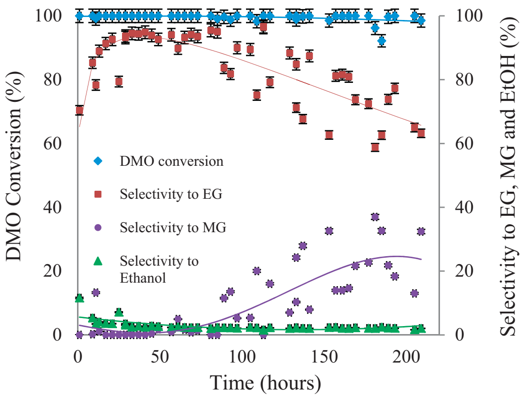

Fig. 8. Stability test of 20Cu-AM30-AC [catalyst mass: 0.3 g Cu, gas condition (pressure: 2 MPa; WHSV: 0.8 g DMO/(h*g cat.); H_2: 92.6 vol.%; N_2: 7.4 vol.%); H_2/DMO mol ratio: 80/1, 230 °C].

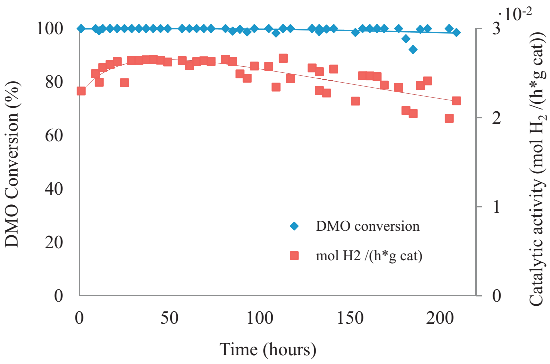

Fig. 9. Stability test of 20Cu-AM30-AC as DMO conversion and catalytic activity to EG + MG + ethanol [catalyst mass: 0.3 g Cu, gas condition (pressure: 2 MPa; WHSV: 0.8 g DMO/(h*g cat.); H_2: 92.6 vol.%; N_2: 7.4 vol.%); H_2/DMO mol ratio: 80/1, 230 °C].

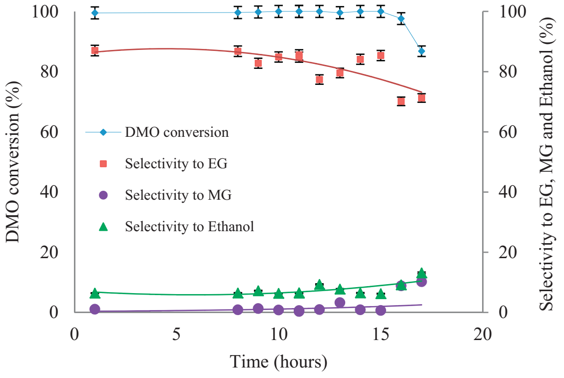

Fig. 10. Stability test of 20Cu-AS30-AE [catalyst mass: 0.3 g Cu, gas condition (pressure: 2 MPa; WHSV: 0.8 g DMO/(h*g cat.); H_2: 92.6 vol.%; N_2: 7.4 vol.%); H_2/DMO mol ratio: 80/1, 210 °C].

support surface available for the AC prepared catalysts, while the AE prepared catalysts have a surface largely occupied by layers of copper and copper compounds (oxides and copper silicates). The more compact structure of AC prepared material seems to ensure a smaller loss of the initial surface area, 28.01% of the original surface compared with 35.45% in case of the AE prepared. In the case of the catalyst 20Cu-AM30-AC, although it is also prepared using AC method, the presence of sodium seems to generate a structure which has a less compact crystallization for copper compounds. This will result in catalyst having a lower initial specific surface, but also having a 22.4% loss of the initial value of specific surface area. In the case of AE prepared catalyst, for which the intention is to create a widespread layer of Cu compounds, thus large surface area available for reaction comparable with the surface of the support, the TEM images show that the main cause of deactivation occurs by sintering of the layer into more compact masses containing Cu [9]. The cause of deactivation for the catalysts prepared using AC method it is more complex. Although they are more thermally stable, as illustrated by the long term tests and TEM images, the detection of

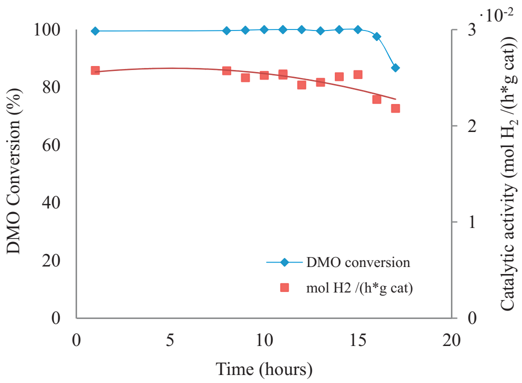

Fig. 11. Stability test of 20Cu-AS30-AE as DMO conversion and catalytic activity to EG + MG + ethanol [catalyst mass: 0.3 g Cu, gas condition (pressure: 2 MPa; WHSV: 0.8 g DMO/(h*g cat.); H_2: 92.6 vol.%; N_2: 7.4 vol.%); H_2/DMO mol ratio: 80/1, 210 °C].

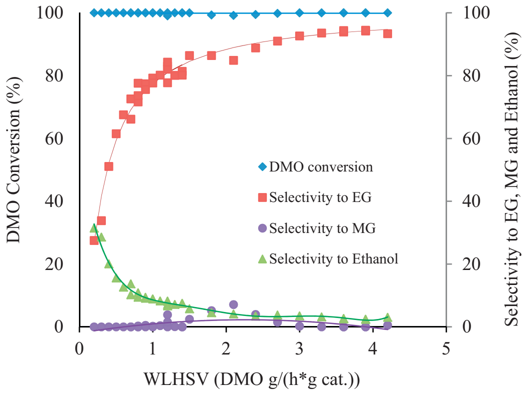

Fig. 12. WLHSV test of 20Cu-AS30-AC [catalyst mass: 0.3 g Cu, gas condition (pressure: 3 MPa; H_2: 92.6 vol.%; N_2: 7.4 vol.%); H_2/DMO mol ratio: 80/1, 210 °C].

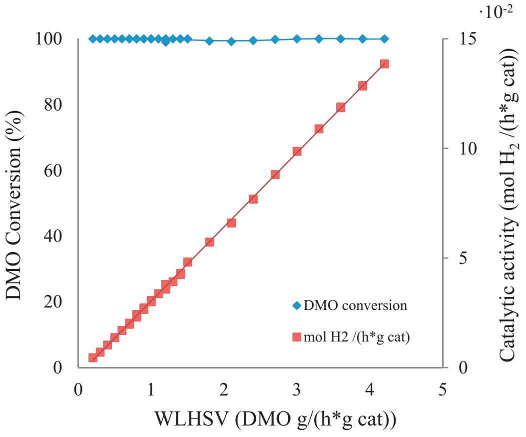

Fig. 13. WLHSV test of 20Cu-AS30-AC as DMO conversion and catalytic activity to EG, MG and ethanol [catalyst mass: 0.3 g Cu, gas condition (pressure: 3 MPa; H_2: 92.6 vol.%; N_2: 7.4 vol.%); H_2/DMO mol ratio: 80/1, 210 °C].

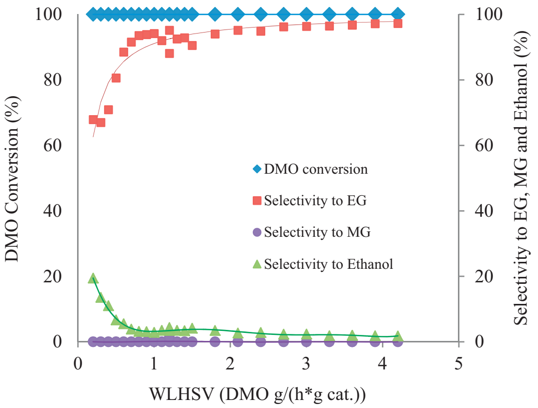

Fig. 14. WLHSV test of 20Cu-AM30-AC [catalyst mass: 0.3 g Cu, gas condition (pressure: 3 MPa; H_2: 92.6 vol.%; N_2: 7.4 vol.%); H_2/DMO mol ratio: 80/1, 230 °C].

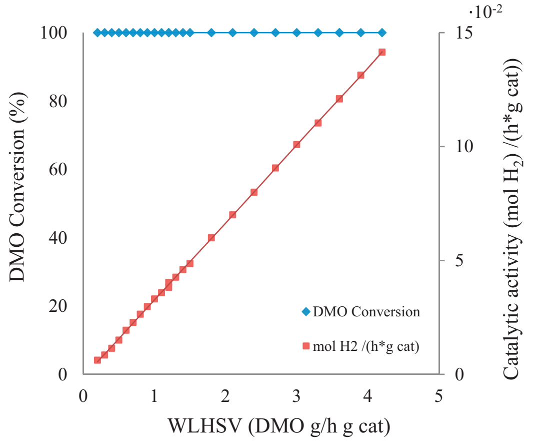

Fig. 15. WLHSV test of 20Cu-AM30-AC as DMO conversion and catalytic activity to EG, MG and ethanol [catalyst mass: 0.3 g Cu, gas condition (pressure: 3 MPa; H_2: 92.6 vol.%; N_2: 7.4 vol.%); H_2/DMO mol ratio: 80/1, 230 °C].

tetramethoxysilane (TMOS) in the product liquid phase indicates dissolution of the support, while the larger presence of Cu^+ in the structure as revealed by XPS/XAES seem to lead to an increase in the thermal stability of the copper structures [33]. According to Wen et al. [21], this type of deactivation by the transformation of the silica support in TMOS is specific to the DMO hydrogenation systems where methanol is used as solvent for DMO, but is improbable for the systems where ethanol is used.

4. Conclusion

The ammonium carbonate precipitation method for synthesis of nanostructured Cu/SiO_2 catalyst for the hydrogenation of dimethyl oxalate (DMO) to ethylene glycol (EG) was successfully developed. It is quicker, safer, and less expensive for preparing nano Cu/SiO_2 catalyst for DMO hydrogenation to EG, an important commercial chemical. The AC based nano Cu/SiO_2 catalysts have similar Cu content, compared to the AE prepared catalyst, but they are characterized by more compacted nanosized crystalline copper structures with more Cu_2O content, which lead to the better DMO conversion and EG selectivity and more thermally stable structures.

Acknowledgements

The authors gratefully acknowledge the support of the U.S. Department of Energy and the State of Wyoming. They also appreciate the great help the members of Dr. Fan's research group that was provided during this research.

Appendix A. Supplementary data

Supplementary data associated with this article can be found, in the online version, at http://dx.doi.org/10.1016/j.apcata.2015.07.026

References

[1] Y. Kong, G. Jiang, M. Fan, X. Shen, S. Cui, A.G. Russell, Chem. Commun. 50 (2014) 12158–12161.
[2] Y. Kong, Xi. Shen, S. Cui, M. Fan, Green Chem. (2015), http://dx.doi.org/10.1039/C5GC00354G
[3] S. Cui, Y. Liu, M. Fan, A.T. Cooper, B. Lin, X. Liu, G. Han, X. Shen, Mater. Lett. 65 (2011) 606–609.
[4] E. Jin, Y. Zhang, L. He, B. Teng, M. Fan, Appl. Catal. A 476 (2014) 158–174.
[5] E. Jin, L. He, Y. Zhang, A.R. Richard, M. Fan, RSC Adv. 4 (2014) 48901–48904.
[6] H. Yue, Y. Zhao, L. Zhao, J. Lv, S. Wang, J. Gong, X. Ma, AIChE J. 58 (9) (2012) 2798–2809.
[7] C. Wen, Y. Cui, A. Yin, K. Fan, W.-L. Dai, ChemCatChem 5 (2013) 138–141.
[8] A. Yin, X. Guo, W.-L. Dai, H. Li, K. Fan, Appl. Catal. A 349 (2008) 91–99.
[9] X. Zhang, B. Wang, Y. Guo, G. Xu, J. Fuel Chem. Technol. 39 (9) (2011) 702–705, ISSN: 0253-2409 CN:14-1140/TQ.
[10] L.-F. Chen, P.-J. Guo, M.-H. Qiao, S.-R. Yan, H.-X. Li, W. Shen, H.-L. Xu, K.-N. Fan, J. Catal. 257 (2008) 172–180.
[11] J. Lin, X. Zhao, Y. Cui, H. Zhang, D. Liao, Chem. Commun. 48 (2012) 1177–1179.
[12] A. Yin, C. Wen, W.-L. Dai, K. Fan, Appl. Catal. B 108–109 (2011) 90–99.
[13] J. Zheng, H. Lin, Y. Wang, X. Zheng, X. Duan, Y. Yuan, J. Catal. 297 (2013) 110–118.
[14] Y. Zhu, X. Kong, X. Li, G. Ding, Y. Zhu, Y.-W. Li, ACS Catal. 4 (2014) 3612–3620.
[15] J. Gong, H. Yue, Y. Zhao, S. Zhao, L. Zhao, J. Lv, S. Wang, X. Ma, J. Am. Chem. Soc. 134 (2012) 13922–13925.
[16] H. Yue, Y. Zhao, S. Zhao, B. Wang, X. Ma, J. Gong, Nat. Commun. 4 (2013) 2339–2346.
[17] T. Toupance, M. Kermarec, C. Louis, J. Phys. Chem. B 104 (2000) 965–972.
[18] A. Yin, X. Guo, W.-L. Dai, K. Fan, Catal. Commun. 12 (2011) 412–416.
[19] H. Lin, X. Zheng, Z. He, J. Zheng, X. Duan, Y. Yuan, Appl. Catal. A 445–446 (2012) 287–296.
[20] F. Li, C.-S. Lu, X.-N. Li, Chin. Chem. Lett. 25 (2014) 1461–1465.
[21] C. Wen, Y. Cui, W.-L. Dai, S. Xie, K. Fan, Chem. Commun. 49 (2013) 5195–5197.
[22] Y. Zhu, S. Wang, L. Zhu, X. Ge, X. Li, Z. Luo, Catal. Lett. 135 (2010) 275–281.
[23] NIOSH Pocket Guide to Chemical Hazards, DHHS (NIOSH) Publication No. 2005-149, 3'rd Printing, NIOSH Publications, Cincinnati, OH, 2007, pp. 15.
[24] L. Lin, P. Pan, Z. Zhou, Z. Li, J. Yang, M. Sun, Y. Yao, Chin. J. Catal. 32 (2011) 957–969.
[25] L. He, X. Chen, J. Ma, H. He, W. Wang, J. Sol-Gel Sci. Technol. 55 (2010) 285–292.
[26] F. Zaccheria, N. Scotti, M. Marelli, R. Psaro, N. Ravasio, Dalton Trans. 42 (2013) 1319–1328.
[27] C.J.G. Van Der Grift, P.A. Elberse, A. Mulder, J.W. Geus, Appl. Catal. 59 (1990) 275–289.
[28] S. Wang, X. Li, Q. Yin, L. Zhu, Z. Luo, Catal. Commun. 12 (2011) 1246–1250.
[29] Y. Huang, H. Ariga, X. Zheng, X. Duan, S. Takakusagi, K. Asakura, Y. Yuan, J. Catal. 307 (2013) 74–83.
[30] Z. He, H. Lin, P. He, Y. Yuan, J. Catal. 277 (2011) 54–63.
[31] A. Lundström, B. Andersson, L. Olsson, Chem. Eng. J. 150 (2009) 544–550.
[32] A.N. Alexandrova, W.L. Jorgensen, J. Phys. Chem. B 111 (4) (2007) 720–730.
[33] Z. Huang, F. Cui, H. Kang, J. Chen, X. Zhang, C. Xia, Chem. Mater. 20 (2008) 5090–5099.
[34] H.-M. Chen, Y.-L. Zhu, G.-Q. Ding, H.-Y. Zheng, Y.-W. Li, J. Fuel. Chem. Technol. 39 (2011) 519–526.
[35] K. Zhong, X. Wang, Int. J. Hydrogen Energy 39 (2014) 10951–10958.
[36] T. Laetsch, R.T. Downs, Abstracts from the 19th General Meeting of the International Mineralogical Association, Kobe, 2006.
[37] C.A. Schneider, W.S. Rasband, K.W. Eliceiri, Nat. Methods 9 (2012) 671.
[38] F. De Chaumont, S. Dallongeville, N. Chenouard, N. Hervé, S. Pop, T. Provoost, V. Meas-Yedid, P. Pankajakshan, T. Lecomte, Y. Le Montagner, T. Lagache, A. Dufour, J.C. Olivo-Marin, Nat. Methods 9 (2012) 690–696.
[39] S. Wang, W. Guo, H. Wang, L. Zhu, S. Yin, K. Qiu, New J. Chem. 38 (2014) 2792–2800.
[40] A.G. Shard, Surf. Interface Anal. 46 (2014) 175–185.